Regularization of Phase Contrast Magnetic Resonance Images Using Optical Flow and Smoothness Constraints

E Bergvall[1,2], K Markenroth[3], E Hedstöm[2], H Arheden[2], G Sparr[1]

[1]Lund Institute of Technology, Lund, Sweden
[2]Lund University Hospital, Lund, Sweden
[3]Philips Medical Systems, Best, Netherlands

Abstract

This paper presents a post processing strategy for myocardial velocity fields obtained by phase contrast magnetic resonance imaging. Such data can be used to track cardiac motion and to calculate strain. The method combines data regularization with optical flow estimation to overcome the partial volume effect in the image acquisition. Validation is performed both in vitro and in vivo and it is shown that the method improves the accuracy of cardiac motion tracking.

1. Introduction

Non-invasive quantitative assessment of regional myocardial function is a clinically important task, as subjective assessment of regional wall motion may suffer from poor intra- and inter-observer agreement. Phase contrast magnetic resonance imaging (MRI) provides time resolved velocity maps of the heart as well as anatomy images. Such data can be used to track myocardial motion and to calculate strain and strain–rate [1].

In order to obtain reliable estimates of myocardial motion and strain, post processing of the measured velocity maps is needed to reduce the effect of measurement noise and image artifacts. Spatial regularization of phase contrast MRI has not been extensively studied. A 3D regularization strategy by divergence minimization has been presented earlier [2], and a 1D strategy by a global smoothness constraint is reported in the literature [3]. In the 2D case, regularization has been performed by projecting the measured velocity field onto piecewise linear functions [4] [5].

In this paper we present a post processing method that uses both velocity maps and anatomy images as well as fundamental properties of MRI image acquisition. This method is validated both in vitro and in vivo by comparison to MRI grid tagging.

2. Methods

2.1. A combined data regularization — optical flow estimation framework

The post processing strategy is based on two important properties of MRI image acquisition;

- The measurement error in the velocity maps is proportional to signal intensity in the anatomy images.
- The received signal from the interfaces between different media will be a mixture of signals, known as the partial volume effect. Therefore the velocity data may be corrupt in such areas.

Optical flow can be defined as the deformation field that warps an image to a subsequent one. Due to the aperture problem, optical flow can only be reliably estimated in areas with sufficient image intensity structure [6]. Thus, it can be used to reduce the partial volume effect as the image gradient is often large on interfaces between different media.

Some notations and definitions are needed in the following. Let the image domain be denoted by $\Omega = [0, M] \times [0, N] \subset \mathbf{R^2}$. Let $\mathbf{Z^2}$ be the sampled plane, with grid points $\mathbf{r} = (i, j), i, j \in \mathbf{Z}$ and let $\Omega_s = \Omega \cap \mathbf{Z^2}$. Let $I_t(\mathbf{r}) \in [0, 1]$ be the anatomy image at time $t = [0, 1, \ldots, T]$. We will evaluate I_t on Ω by interpolation on Ω_s. If f is a function on $\mathbf{R^2}$, let f_s denote its sampling to $\mathbf{Z^2}$. Let $f * g$ and $f_s * g_s$ denote continuous and discrete convolutions, respectively, and let $f_s \cdot g_s$ denote componentwise product of f_s and g_s. Let $\mathbf{v}_t(\mathbf{r})$ be the measured velocity field at time t. Define a coefficient function as

$$\text{Ш}_{\mathbf{c}} = \mathbf{c}(\mathbf{r}) \cdot \sum_{i=1}^{\lfloor M/\Delta_x \rfloor} \sum_{j=1}^{\lfloor N/\Delta_y \rfloor} \delta(\mathbf{r} - (i\Delta_x, j\Delta_y)),$$

where δ is the Dirac delta, Δ_x and Δ_y are integers and $\mathbf{c}(\mathbf{r})$ takes real values. Denote by $\mathbf{u}_t(\mathbf{r})$ the regularized velocity field sought for. Let $g(\mathbf{r})$ be a smoothing kernel. Claiming smoothness and that constant sampled velocity field should

stay constant after interpolation, $\mathbf{u}_t(\mathbf{r})$ is represented by

$$\mathbf{u}_t(\mathbf{r}) = N(\mathbf{r}) \cdot (\mathrm{III}_{\mathbf{c}} * g(\mathbf{r})),$$

where convolution is applied separately to each component of the vector. The normalization function $N(\mathbf{r})$ is defined as

$$N(\mathbf{r}) = \frac{1}{\mathrm{III}(\mathbf{r}) * g(\mathbf{r})},$$

where III is the first component of $\mathrm{III}_{\mathbf{c}}$ evaluated with $\mathbf{c} = 1$. It is required that the support of the smoothing kernel is large enough so that $\mathrm{III} * \mathrm{g} > 0$ is satisfied for all $\mathbf{r}$ which establishes a condition on Δ_x and Δ_y once the kernel is chosen. It is also required that Δ_x and Δ_y are chosen to be greater than 1, otherwise any function sampled on Ω_s can be represented by $\mathbf{u}(\mathbf{r})$.

Data regularization and optical flow estimation is performed by finding the function $\mathbf{c}$ that minimizes the functional

$$E(\mathbf{u_t}) = \sum_{\mathbf{r}\in\Omega_s} (\mathbf{u}_t(\mathbf{r}) - \mathbf{v}_t(\mathbf{r}))^2 \cdot W_{\text{data}}(\mathbf{r}) +$$

$$(I_{t+1}(\mathbf{r}+\mathbf{u}) - I_t(\mathbf{r}))^2 \cdot W_{\text{optical}}(\mathbf{r}),$$

where W_{data} and W_{optical} are positive weight functions to be defined later.

The minimum can be found iteratively by a gradient descent equation

$$\mathbf{c}^{(k+1)} = \mathbf{c}^{(k)} - \mathrm{III} \cdot (N \cdot ((\mathbf{u_t}^{(k)} - \mathbf{v}_t) \cdot W_{\text{data}} +$$

$$(I_{t+1}(\mathbf{r} + \mathbf{u}^{(k)}) - I_t(\mathbf{r})) \cdot \nabla I_{t+1}(\mathbf{r}) \cdot W_{\text{optical}})) * g,$$

where k serves as the iteration counter. The approximation $I(\mathbf{r}+\mathbf{u}) \approx I(\mathbf{r}) + \nabla I \cdot \mathbf{u}$ was used when deriving the above equation. This scheme is straightforward to implement as it only uses convolutions and image interpolation. We will let $g(\mathbf{r})$ be a truncated Gaussian kernel with standard deviation σ.

The weight functions used above were constructed with the two image acquisition properties in mind. The functions were normalized so that $W_{\text{data}} \in [0, 1]$ and we define $W_{\text{optical}} = 1 - W_{\text{data}}$. The data attachment weight function was defined as

$$W_{\text{data}}(\mathbf{r}) = \frac{I(\mathbf{r})}{1 + \lambda |\nabla I(r)|^2},$$

where $\lambda > 0$ is a tuning parameter. Thus, optical flow estimation is used in areas with low signal intensity, even if it is a homogenous area. This will imply that the regularized velocity field will be close to zero in such areas.

The post processing method was implemented in MATLAB (Mathworks).

2.2. Image acquisition

The post processing scheme was validated using both in vitro and in vivo data.

The phantom consisted of an Agarose-gel, cast in a plastic container. The size of the phantom was 8×8×5 cm^3, and the approximate T_1-value of the gel was 800 ms. In the scanner, the phantom was placed on a small plastic cart which restricted the motion a rigid translation. Forward-backward motion of the phantom was accomplished by connecting the front of the cart to a rotating disc, using a thin wire. Each turn of the disc pulled the cart with the phantom forward, while a rubber band returned it to the original position. The phantom is shown in Figure 1. The amplitude of the phantom motion was 19 mm and the period of the motion was 1.07 s.

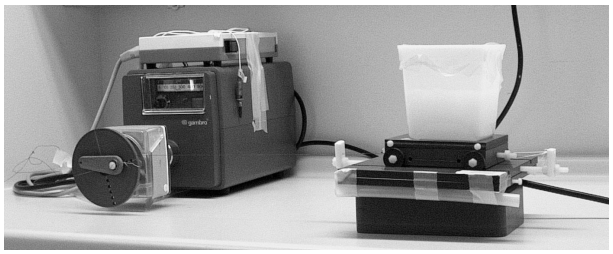

Figure 1. Image showing the phantom on the moving cart and the wire connection to the rotating disc. The angular velocity of the disc is controlled by a signal generator.

Data from a total of $n = 10$ human subjects was acquired in long axis slices, after informed consent.

Velocity data was acquired using a 1.5 T Gyroscan Intera Scanner (Philips Medical Systems). Spatial resolution was 1.2x1.2 mm in vitro and 1.5x1.5 mm in vivo with a slice thickness of 8 mm and temporal resolution of 25-35 frames/heartbeat. Typical imaging parameters were TR=24 ms, TE=5.3 ms, v_{enc}=0.30 m/s, flip angle 20°, matrix size 256×192 pixels and FOV = 400 mm × 300 mm. In the in vivo case saturation bands were used to reduce the signal from blood [7]. Retrospective ECG gating was used when reconstructing the images.

In the in vivo case, saturation grid tag images were acquired in the same imaging plane. Typical parameters were TR=3.8 ms, TE=1.8 ms, , flip angle = 15°, saturation tag gap = 7 mm, matrix size = 256×192 pixels, FOV 400 mm× 300 mm, temporal resolution of 12 frames/heartbeat.

2.3. Data analysis

The performance of the post processing scheme was validated by calculating the displacement field by temporal integration of the velocity field and comparing it to the true displacement field. In the in vivo case the true displacement field was only sparsely estimated by manual tracking of grid tag intersections. The root mean square error was used in the comparison. Three different settings were used in the experiment; one with no regularization at all, one with $W_{\text{data}} = 1$ and W_{optical}=0 and finally one with the weight functions described above.

The grid spacing was set to 3 pixels and the discrete Gaussian kernel had a standard deviation of 3. The parameter λ in the weight functions was experimentally set to 10 and a maximum of 100 iterations was used.

3. Results

Figure 2 shows the error when tracking the phantom motion using the three different settings.

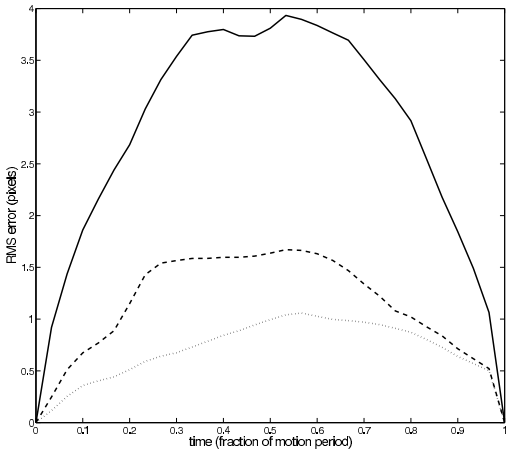

Figure 2. RMS error for motion tracking with no regularization (solid), regularization of velocity measurements only (dashed) and using combined data regularization — optical flow estimation scheme (dotted).

Figure 3 shows the results of the in vivo study as a boxplot where the mean error during the cardiac cycle was used for comparison. The differences between the three settings are statistically significant ($p < 0.005$) based on a paired t-test.

A qualitative evaluation is shown in Figure 4 where the displacement field at end systole is shown with and without regularization.

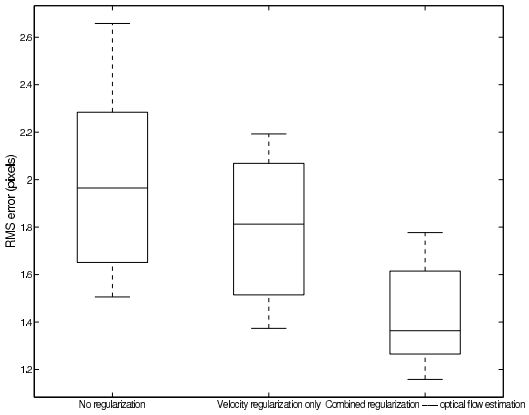

Figure 3. Boxplot for motion tracking in the in vivo case using three different settings.

4. Discussion and conclusion

We have constructed and validated a post processing scheme for 2D phase contrast MRI that takes both the measured velocity field and the anatomy images into account. The method is based on fundamental properties of phase contrast image acquisition and assumes that the myocardial velocity field is smooth. The method improved the accuracy in motion tracking in all cases, both in vitro and in vivo. It was also shown that regularization using only velocity data improved the result, but not as much as the combined regularization — optical flow estimation scheme. This suggests that all information acquired using phase contrast MRI should be taken into account in order to regularize the data.

An advantage of the proposed method is that no image segmentation is needed. Segmentation of phase contrast MRI is time consuming and difficult even if manual segmentation is used.

Validation in the in vivo case was made by comparison to saturation grid tag images which were manually analyzed. This will only give a sparse estimation of the displacement field which will be somewhat unreliable at the end of the cardiac cycle due to tag fading. It is also difficult to track tag intersections close to the epi- and endocardium which may cause the effect of the optical flow estimation to be less pronounced.

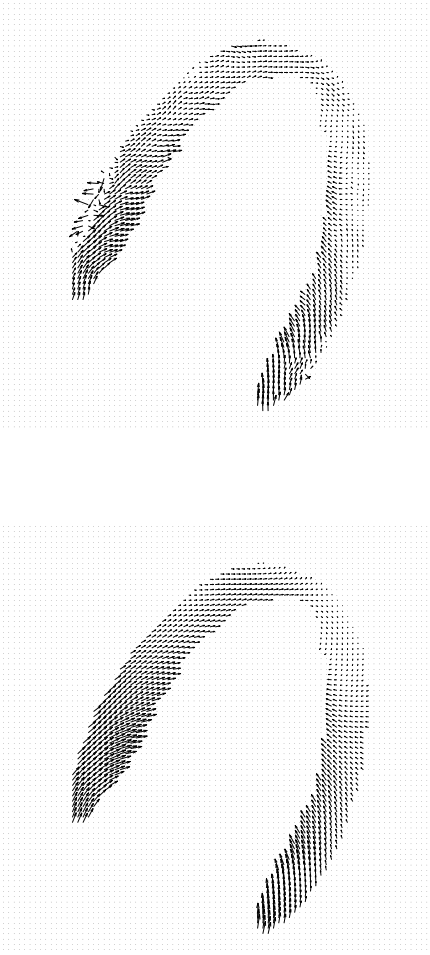

Figure 4. Myocardial displacement field at end systole using no regularization (top) and with combined regularization — optical flow estimation (bottom). Note especially the differences at the epicardium.

The method extends naturally to 3D which may be used for research purposes but not in clinical routine due to the long acquisition time of such measurements.

We conclude that the constructed post processing scheme improves the accuracy of cardiac motion tracking. The lack of user interaction will increase the potential for clinical use of 2D phase contrast MRI.

Acknowledgements

This work was supported by the Swedish National Heart — Lung Foundation.

References

[1] Masood S, Yang G-Z, Penell D, Firmin D. Investigating intrinsic myocardial mechanics: The role of MR tagging, velocity phase mapping, and diffusion imaging. Journal of Magnetic Resonance Imaging 2000;12:873–883.

[2] Buonocore M. Algorithms for Improving Calculated Streamlines in 3-D Phase Contrast Angiography. Magnetic Resonance In Medicine 1994;31:22–30.

[3] Herment A, Mousseaux E, de Cesare A, Jolivet O, Dumee P, Todd-Pokropek A, Bittoun J. Spatial Regularization of Flow Patterns in Magnetic Resonance Velocity Imaging. Journal of Magnetic Resonance Imaging 1999;10:851–860.

[4] Meyer F, Constable T, Sinusas A, Duncan J. Tracking Myocardial Deformation Using Phase Contrast MR Velocity Fields: A Stochastic Approach. IEEE Transactions on Medical Imaging 1996;15:453–465.

[5] Zhu Y, Pelc N. A Spatiotemporal Model of Cyclic Kinematics and its Application to Analyzing Nonrigid Motion with MR Velocity Images. IEEE Transactions on Medical Imaging 1999;18:557–569.

[6] Beauchemin S, Barron J. The Computation of Optical Flow. ACM Computing Surveys, 1995;27:433–467.

[7] Drangova M, Zhu Y, Pelc N. Effects of artifacts due to flowing blood reproducibility of phase-contrast velocity data. Journal of Magnetic Resonance Imaging, 1997;7:664-668.

Address for correspondence:

Erik Bergvall
Department of Clinical Physiology
Lund University Hospital
S-22185 Lund
Sweden
erik.bergvall@med.lu.se